NASA HuLC Fluid Transfer Team

CQC: Cryogenic Quick Connection

Submitted by: Colin Wall, Undergraduate, Mechanical Engineering
Vianca Nerona, Undergraduate, Mechanical Engineering
Griffin Vernon, Undergraduate, Mechanical Engineering
Monica Herrington, Undergraduate, Mechanical Engineering
Ethan Hook, Undergraduate, Mechanical Engineering
Thomas Breen, Undergraduate, Mechanical Engineering

Senior Project
Sponsor: *John Chen*
California Polytechnic University
San Luis Obispo
College of Engineering

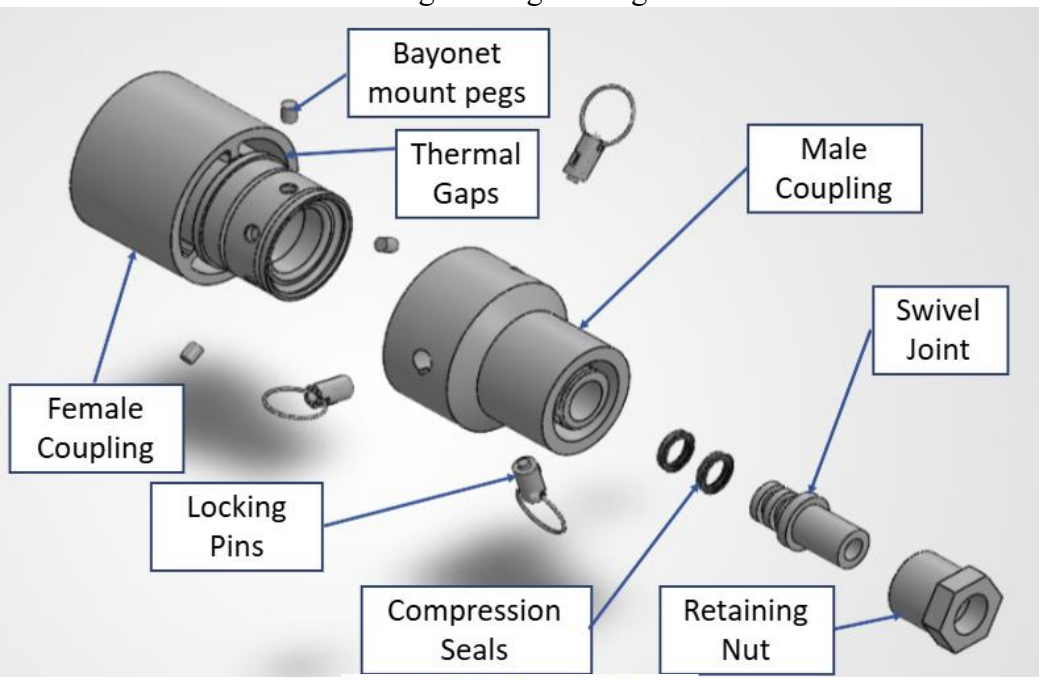

Mechanical Engineering
CAL POLY

Cal Poly Fluid Transfer Team, Cryogenic Quick Connect

Fluid Transfer Between Surface Assets on the Moon and Mars

- Design a fluid coupling that is universal to all NASA surface assets
- Emphasize safety and reliability
- Focus on ergonomics for ease of use by astronauts and robots
- Account for hazards introduced by harsh lunar and Martian environments

Key Design Details & Innovations of the Concept

- Bayonet locking mechanism
- Redundant pin safety mechanism
- Thermal protection gap
- Robust cone shaped fitting aids ergonomics

Summary of Schedule & Costs for the proposed solution's path to adoption

- Solution's path to adoption will take about 6 years
  - Year 1: Finalize material selection and validate design through simulations
  - Years 2-3: use EDUs to validate prototype through environmental simulations
  - Years 4-6: Manufacture refined design, run qualification tests, and integrate with HLS architecture
- Costs: $133.56/unit [STEEL] or $348.56/unit [Ti-3Al-2.5V]

Table of Contents

Executive Summary

NASA aims to establish a permanent base on the moon that supports human life while preparing for long-duration missions to Mars. Reliable fluid transfer between surface assets is critical to astronaut survival and overall mission success. The Cryogenic Quick Connection (CQC) is a fluid coupling designed to provide safe, reliable transfer of multiple fluids in harsh extraterrestrial environments across NASA surface systems.
The CQC consists of a fixed male end and a free female end, interlocked via a conical bayonet locking mechanism with redundant locking pins to ensure structure integrity and leak prevention. The conical interface geometry facilitates alignment and engagement for human operators and robotic systems, reducing connection time and operational complexity.
Thermally, the CQC mitigates extreme environmental heat loads through integrated vacuum insulation and low solar absorbance coating. Its ergonomic, fail-safe design minimizes opportunities for fluid loss, enhancing operational safety and crew confidence during routine surface operations.

Problem Definition

NASA's Artemis campaign will deploy astronauts throughout the moon and establish a base to further scientific discovery, improve technology, and prepare for an eventual mission to Mars [1]. In establishing a base that can support human life, fluid transfer systems must be developed to facilitate the transfer of a variety of fluids between surface assets. Water and liquid oxygen will need to be resupplied to astronaut habitats as they are essential to human life. Astronaut waste needs to be removed from habitats to maintain quality of life. Fuel transfer is necessary for powering ships used to traverse the moon as well as powering vital subsystems in the habitats.
The harsh Martian and lunar environments introduce significant engineering challenges in fluid transfer due to the combination of vacuum exposure, extreme thermal cycling, reduced gravity, and pervasive regolith contamination. During transfer, the vacuum environment makes cryogenic fluids susceptible to continuous boil-off from radiative heat leaking into the fluid and flash vaporization during pressure transitions [2]. To add on, the vacuum environment eliminates the possibility of convective heat transfer, adding a constraint to thermally managing a system. Surface temperatures ranging from 96 to 391 kelvin around the moon's equator induce severe thermal expansion and contraction cycles [3]. The thermal fluctuations will also degrade seal structural interfaces over time. Additionally, regolith, harmful moon dust, is present all over the moon. Regolith can infiltrate a fluid transfer system and accelerate wear and tear while increasing the risk of leakage.
NASA needs a standardized system that can mitigate all these issues over multiple repeated cycles. A standardized system will reduce complexity in lunar base operations by creating a plug-and-play architecture. Having a single method of fluid transfer will reduce the logistics burden on humans or robots that would have to understand how to deal with multiple, sophisticated fluid transfer systems. Furthermore, standardization will empower NASA to scale their operations on the moon faster than if they had to train astronauts and robots on a new system for each sub-base. Establishing a standardized system to transfer fluids is therefore essential to enabling a sustainable and extensible lunar architecture.

Design Description

Below in Table 1 is a list of all the critical specifications, and the justification for how we are meeting them. These specifications have been selected based on NASA standards for lunar and Martian environments, as well as standards in industry for fluid couplings.
NASA, and the astronauts that NASA is charged with keeping safe, face the challenge of reliably, conveniently, and safely transferring a wide range of fluids between surface assets on the Lunar and Martian surfaces. Our design focuses on the interface between assets, allowing astronauts to easily connect assets together to transfer a wide range of fluids, including cryogenics. It does this with some key features. The first feature is the bayonet locking mechanism.

The bayonet locking mechanism, shown below in Figure 1, allows for quick and simple rotation locking for the astronaut. Furthermore, the indentation at the end of the lock motion means that any axial loads from fluid pressure are adequately supported by the locking lugs, and importantly, that pressurization prevents the bayonet locking mechanism from rotating, as the pressure forces the locking lugs into the indentation.

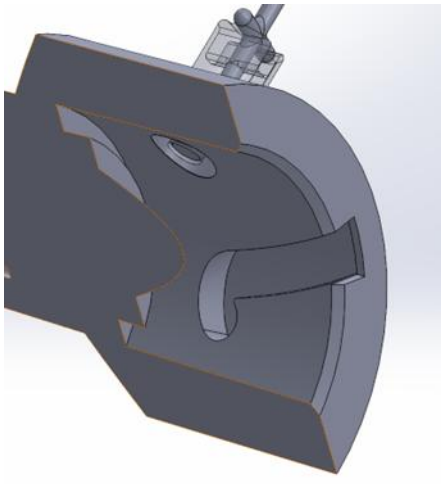

Figure 1. View of bayonet locking channel.

The next design element that contributes to astronaut safety is the three radial locking pins. Three spring loaded plungers are inserted after the coupling is connected, lowering shear pins between the two halves of the coupling. These are intended to prevent any rotation after the coupling is connected. These are redundant safety measures, as the bayonet system should prevent rotation inherently.

An element to assist in ease of use as well as improve the robustness of the design is the cone shaped interface between the couplings, shown in Figure 2. This allows the couplings to more easily self-align, aiding astronauts in conditions with decreased dexterity.

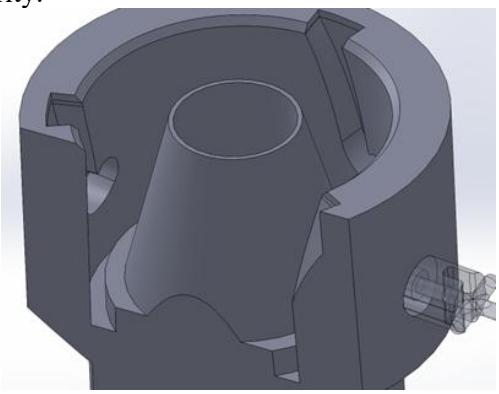

Figure 2. Cutaway view of cone interface, male coupling.

Our last key design feature is the thermal gap integrated within the coupling. The lunar environment coupling with cryogenic flow, can create large temperature differentials. This gap is intended to prevent these large temperature swings from creating excessive thermal stresses, as well as allow for easier handling of the coupling after cryogenic flow.

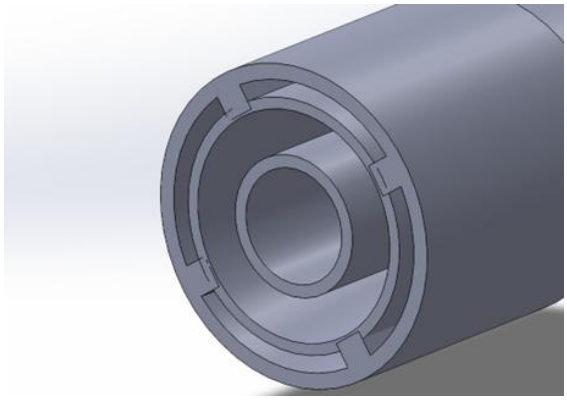

Figure 3. Thermal gaps.

Finally, while our design is not finalized, we intend to meet or exceed all the following specifications identified in Table 1.

Table 1. Design Specifications

#	Spec	Specification Description	Justification
1	Pressure: 1000 psi	This is the maximum pressure that the coupling will experience under normal operating conditions.	While traditional O-rings are not rated for these pressures, spring energized seals like the ones we will install are rated for pressures up to 3000psi when properly installed.
2	Environmental Temperature: –173°C to +127°C	This is the range of temperatures on the surface of the moon.	The vacuum insulated design prevents the conductive heating of critical inner sealing surfaces, while an external radiative coating limits the amount of incident radiation absorbed.
3	Propellant Temperatures: -183°C	This is the lowest temperature of fluid that will flow through the coupling.	While our prototype will be made of aluminum, the final specification will be for a metal, most likely stainless steel, that is currently used in industry for cryogens.
4	Connection Force: 60 N	This is the force required to connect the coupling.	The primary opposing force to connect the coupling is the seal. Spring energized seals have a low modulus, and our small displacement will ensure low locking force. This meets the NASA specification for one-hand pull limits.
5	Seal Displacement: 1.25 mm	The displacement of the O-ring for proper sealing.	Based on our coupling size, the Parker O-Ring Handbook specifies 1.25 mm of displacement.
6	Flow Coefficient: >200	Coupling must achieve a flow coefficient such that it ensures a low-pressure drop and efficient propellant transfer.	The internal geometry is designed with a smooth, enlarged flow path that minimizes turbulence, allowing the coupling to reach a flow coefficient above 200 in simulation.
7	Mass: <12 kg per side	The mass of the male or female side of the coupling individually.	The mass of our initial prototypes, as well as SolidWorks mass properties calculations, show 8kg for both sides.

Analysis

Fluid Hand Calculations

A first-order analytical model was developed to estimate Reynolds number, friction factor, pressure drop across the coupling, and equivalent flow coefficient (C_v). This analysis establishes baseline hydraulic performance prior to higher-fidelity modeling and supports downstream structural and seal load evaluations.

Results of Pressure Drop

Calculated pressure drops can be seen in Table 2 for the 5 in straight coupling section (D = 0.75 in).

Table 2. Pressure Drops for Different Fluids

#	Fluid	ΔP (psi)	C_v
1	Air (20°C)	0.0377	1.43
2	Water (20°C)	0.374	49.1
3	Liquid Hydrogen (20 K)	0.0206	55.7
4	Liquid Oxygen (90 K)	0.331	55.7
5	Sludge (2% Solids)	0.862	32.5
6	Sludge (10% Solids, Worst Case)	80.9	3.43

For assumptions and modeling methodology, see Appendix D.

Recommended Refinements

Further detailed CFD analysis could be done to confirm the hand calculations. This refinement can be completed within an estimated 8–10-week timeframe.

Axial Force and Seal Compression Analysis

A closed-form analytical model was developed to estimate axial hydraulic forces acting on the coupling and resulting seal compression. With a maximum allowable seal displacement of $\delta_{seal,max} = 1.25$ mm, the axial load needed to properly compress the seal was found to be: $F_{axial,max} = 2.52$ kN. This load case was carried forward into seal compression analysis and structural FEA to ensure conservative evaluation of coupling integrity.

Results of Seal Compression Finite Element Analysis

A dedicated finite element analysis was performed using the maximum axial seal load of 2.52 kN derived from the pressure-based hand calculations. The objective was to evaluate seal deformation, stress distribution, and margin relative to the allowable compression limit.

Results indicate that maximum seal displacement remained below the 1.25 mm allowable limit. Stress distribution across the annular cross-section was uniform, with no localized overstressing predicted under static compression. The numerical results correlate well with analytical estimates, providing confidence in the load derivation and modeling approach. Overall, the seal maintains deformation within elastic limits while providing sufficient compression margin without risk of excessive extrusion under the evaluated load case.

Recommended Refinements

To further mature the seal design, additional analysis may be conducted in the future, including thermally coupled modeling to evaluate performance under cryogenic and transient temperature conditions, as well as long-duration compression creep assessment. These refinements can be completed within an estimated 8–12-week timeframe and would support progression toward environmental qualification readiness.

Finite Element Analysis (FEA) – Coupling Structure

A linear static finite element analysis was conducted to evaluate structural response of the coupling under worst-case internal pressure loading. The objective of this analysis was to verify structural integrity, quantify stress distribution, and establish margin relative to material yield strength.

Loading and Boundary Conditions

The FEA model applied the maximum internal pressure condition corresponding to the previously defined worst-case hydraulic scenario (1000 psi). Internal pressure was applied uniformly to all wetted internal surfaces of the coupling body. Axial reaction forces generated by pressure were inherently captured through the pressure loading distribution. Appropriate constraints were applied at the mechanical interface locations to represent attachment to the mating structure while avoiding artificial over-constraint. The study was conducted in Abaqus 2025, using an axisymmetric sketch of the channel profile. The element type used was CAX4I, and 7043 elements were used for the 2-D profile.

The analysis assumed:

- Linear elastic material behavior
- Isotropic material properties
- Static loading
- No thermal loading

Mesh and Model Considerations

A refined mesh was applied in regions of geometric discontinuity, including:

- Fillets
- Retention features
- Seal grooves

Global mesh sizing was selected to ensure stress convergence while maintaining computational efficiency.

Results of Structural Response

Figure 4 shows the resulting von mises stress contour plot of the 2-D profile swept 180 degrees.

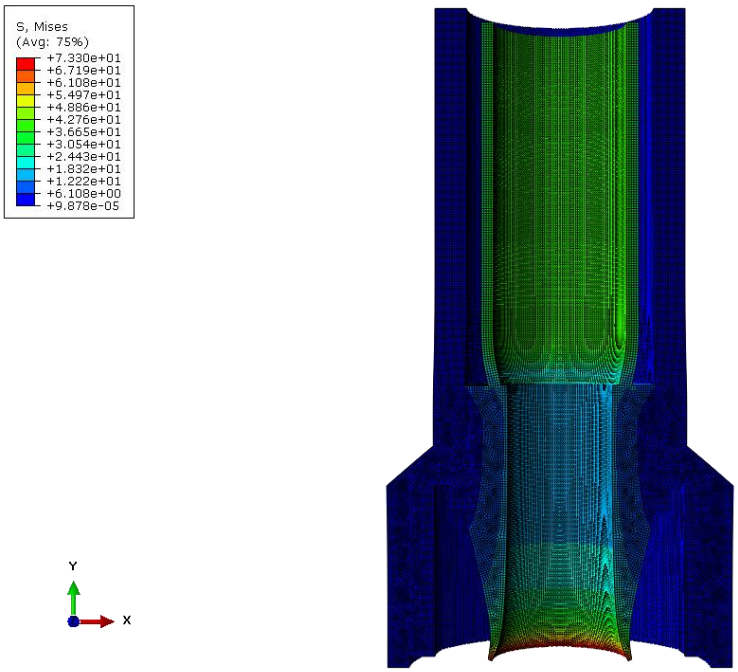

Figure 4. Contour plot of Von Mises stress in deformed coupling imparted through a pressure load

Table 3 displays the data acquired from the pressure study.

Table 3. Structural Response from the Coupling FEA Study

#	**Parameter**	**Result**
1	Maximum von Mises Stress	73.3 MPa
2	Location of Peak Stress	Edge of Male Cone connector
	Material Yield Strength	350 MPa
3	Factor of Safety (Yield)	4.77
4	Maximum Displacement	3.8 μm

Design Implications

The FEA results confirm that the CQC coupling body can safely withstand the worst-case internal pressure loading of 1000 psi. The maximum stress of 73.3 MPa in the coupling was found at the edge of the aligning cone, while the representative stress in the longer fluid channel averaged around 42.76 MPa. These stresses resulted in a safety factor of 4.77 and 8.18 for maximum and representative stress, respectively. The high safety factor from the representative stress gives the coupling a substantial structural margin for load cases not captured in this analysis. A thermally coupled study will need to be completed during phase 1 of the path-to-flight plan to quantify the contribution of stress from lunar surface temperature cycling. Additionally, the maximum displacement of 3.8 μm at the edge of the conical shape is negligible relative to the 1.25 mm seal compression allowable, confirming the structural deformation under pressure will not compromise the sealing geometry. Other than the thermal-load case discussed, further FEA studies should investigate contact stress at the bayonet lugs, the fatigue life of the coupling to verify its operational life, as well as a heat transfer study that can quantify effectiveness of the air channel in reducing heat transfer between the outside of the coupling and the internal fluid channel.

Preliminary Casting Evaluation

Initial investment casting trials using standard PLA-based 3D printed patterns (Aluminum A356) were conducted to assess manufacturability of the coupling geometry. These attempts revealed manufacturing limitations affecting structural integrity and surface quality. Observed issues included cracking of the investment mold during burnout, internal void formation, and surface defects in critical sealing regions. Root causes were identified as incomplete PLA burnout, ash residue contamination, and thermal expansion mismatch between the pattern and investment material. These results indicate that PLA patterns are not suitable for high-fidelity casting of this geometry, particularly where sealing surfaces and dimensional tolerances are critical. Future iterations will utilize Siraya Tech high-resolution resin to improve burnout quality and surface finish.

Production Tooling Considerations

Preliminary industry feedback indicates that production tooling for precision investment casting of this geometry would require approximately 10 weeks of lead time and an estimated $50,000 in upfront cost for medium-volume production (vendor estimate, 2026). This is consistent with industry experience that precision tooling represents a significant early investment and schedule driver prior to production casting.

Proposed Path-to-Flight Plan

The CQC has demonstrated analytical feasibility through fluid modeling, seal compression analysis, and structural FEA. The following phased development plan outlines the steps required to advance from the current prototype to a flight-certified connector.

Table 4. Outline of the Proposed Path-to-Flight Plan

Phase	Timeline	Key Activities	Deliverables
I – Design Closure	Year 1	Finalize material selection (316 SS vs. Ti-3Al-2.5V); complete thermally-coupled FEA across lunar temperature range (96–391 K); run CFD to validate C_v and pressure drop; qualify resin-pattern investment casting process	Material selection memo; updated FEA report; CFD C_v validation; casting process report
II – Prototype Validation	Year 2	Fabricate Engineering Development Units (EDUs) in flight-intent material; conduct ambient flow testing (water at 30 GPM); perform helium leak test at 1000 psi; proof pressure test; bayonet torque verification; regolith contamination test with lunar dust simulant	Flow test report; leak test report; proof test report; contamination test report
III – Environmental Qualification	Year 3	Thermal vacuum (TVAC) cycling across full lunar temperature range; random vibration and shock testing; 100-cycle thermal cycling at cryogenic temperatures; long-duration seal creep test (1000 hr at operating pressure)	TVAC report; vibration/shock report; thermal cycling report; seal creep data
IV – Flight-Like Hardware	Years 4–5	Manufacture qualification and flight units in production tooling; acceptance testing on each unit; CMM dimensional inspection; human factors validation with suited operator connect/disconnect	Acceptance test records; inspection reports; human factors report
V – Integration & Deployment	Year 6+	System-level integration with HLS fluid transfer architecture; crew training; final certification	Certification data package; crew training materials

Qualification Testing

To advance the CQC from its current prototype stage to flight readiness, the following qualification tests are planned. These tests verify that the connector can perform reliably under the conditions it will face on the lunar surface.

Table 5. Planned Qualification Tests

Test	Purpose	Pass Criteria
Proof Pressure	Confirm structural integrity at 1.5× operating pressure	No leakage or permanent deformation
Helium Leak Test	Verify seals are tight enough for cryogenic service	Leak rate ≤ 1×10^{-6} scc/s
Flow Coefficient (C_v) Test	Measure actual pressure drop and compare to $C_v \geq 200$ spec	Measured C_v meets or exceeds specification
Connect/Disconnect Cycle Life	Confirm connector holds up over repeated EVA use	No degradation in sealing after 500 cycles
Regolith Contamination	Verify connector functions after exposure to lunar dust (JSC-1A simulant)	No increase in leak rate; bayonet mechanism operates normally
Thermal Vacuum (TVAC)	Simulate the lunar environment — temperature extremes in vacuum	Connector seals and latches normally after 10 thermal cycles
Cryogenic Leak Test	Confirm sealing performance at LO_2 temperatures (−183°C)	No visible leakage during LN_2 flow
Bayonet Torque at Temperature	Verify locking mechanism doesn't bind or loosen at cryogenic temperatures	Engagement torque within ±20% of ambient baseline

Note: CFD validation of the internal flow geometry is also planned in Phase I to resolve the discrepancy between the hand-calculated C_v (49–56) and the specification of $C_v \geq 200$. This will clarify whether the spec applies to this connector size or if the internal geometry needs to be revised.

Risk Summary

The following table identifies the key risks associated with advancing the CQC to flight readiness and our planned mitigations.

Table 6. Outline of Key Risks of the CQC

Risk	Likelihood	Severity	Mitigation
Lunar dust contaminates sealing surfaces	High	High	Add dust cap or wiper seal to design; test with JSC-1A simulant in Phase II
Calculated C_v (49–56) doesn't meet $C_v \geq 200$ spec	High	Medium	Run CFD in Phase I to identify source of discrepancy; revise internal bore geometry if needed
Investment casting defects on sealing surfaces	Medium	High	Transition to resin-pattern casting (Siraya Tech); keep machined billet as fallback option
Bayonet mechanism binds at cryogenic temperatures due to thermal contraction	Medium	High	Include cryogenic torque testing in Phase II; update clearances in design if binding observed
Spring-energized seal properties unknown at −183°C	Medium	High	Source cryogenic material data from seal vendor (e.g., Bal Seal, Greene Tweed); update FEA with real data
14-week tooling lead time causes schedule delays	Medium	Medium	Use machined billet EDUs in Phase II to allow design iteration before committing to production tooling

Budget

The projected budget for full-scale production assumes the final coupling could be manufactured from either Stainless Steel or Titanium using ceramic investment casting to achieve the required accuracy, material properties, and surface finish for high-pressure application. Post-casting machining and inspection would be required to meet aerospace tolerances. Critical components such as spring-energized seals and specialty springs would be sourced from qualified aerospace suppliers to ensure compliance with pressure, temperature, and vacuum requirements. Cost estimates are shown below in Tables 7 and 8.

Table 7. Cost for 1,000 units using 316 Stainless

Item	Cost per Unit	Amount	Extended Cost
PTFE Spring Energized Seal	$36.06	1000	$36,060
Springs	$2.50	3000	$7,500
316 Stainless Steel	$5.00 / kg	8000	$40,000
Mold	$50,000	1	$50,000
Total Cost			**$133,560**

Table 8. Cost for 1,000 units using Ti-3Al-2.5V Titanium

Item	Cost per Unit	Amount	Extended Cost
PTFE Spring Energized Seal	$36.06	1000	$36,060
Springs	$2.50	3000	$7,500
Ti-3Al-2.5V Titanium Alloy	$30.00 / kg	8000	$240,000
Mold / Tooling	$65,000	1	$65,000
Total Cost			**$348,560**

While this analysis doesn't include other overhead or manufacturing costs, this gives us a rough estimate for the cost of this program for a moderately sized production run. This gives us a cost per unit of $103.94 for Stainless Steel and $348.6 for Titanium.

Material Selection

The Titanium alloy chosen for the CGC is based on current aerospace industry practice and its increase in titanium usage. Titanium's strength-to-weight ratio is a valuable quality which allows for reliable design without adding mass concerns which an alternate metal, such as steel, might. While Aluminum alloys can have similar properties in terms of being lightweight and strength retention, Titanium is lighter, stiffer, and has great corrosion resistance properties. Ti-3Al-2.5V specifically is used in cryogenic conditions, as it can withstand low temperatures without losing valuable properties; this alloy accounts for fracture toughness and ductility at liquid nitrogen temperatures without the low-temperature embrittlement concerns associated with higher-aluminum titanium alloys. [5]

Dust Mitigation

Lunar dust is a major issue to fluid transfer as it risks contaminants, for protection while the device is not in use and disconnected a cap is put in place. When the coupling is used, the caps are then mated to each other to prevent contamination of the caps. This system is simple and accomplishes the protection. The performance of an iris system was discussed but the complexity of the system risked jams and additional points for breakage which could result in complex maintenance. The caps are a simple system and are easily replaceable over time with wear. These caps maintain the same sealing mechanisms as the coupling system.

Conclusion

The Cryogenic Quick Connection (CQC) shows strong early feasibility as a standardized lunar fluid-transfer interface. Structural FEA confirms the coupling can withstand 1000 psi with a 4.77 safety factor, and seal compression analysis shows deformation remains well below the 1.25 mm allowable, ensuring reliable sealing under load. Fluid hand calculations indicate low pressure drop for water and cryogens, though the gap between the calculated C_v (≈49–56) and the $C_v \geq 200$ requirement remains a key design item for Phase I CFD validation.

Manufacturability studies highlight the need to transition from PLA to resin-pattern casting, with machined billet prototypes supporting near-term testing. With targeted refinements in thermal modeling, flow-path optimization, and casting process development, the CQC is well-positioned to progress through the proposed path-to-flight plan and mature into a flight-ready connector for NASA’s lunar interface operations.

Appendix A: References

[1] NASA, “Artemis: Humans in Space,” https://www.nasa.gov/humans-in-space/artemis/

[2] W. L. Johnson and J. R. Stephens, “NASA’s Cryogenic Fluid Management Technology Development Roadmaps”, NASA Technical Reports Server, 2019. https://ntrs.nasa.gov/api/citations/20190000305/downloads/20190000305.pdf

[3] National Aeronautics and Space Administration (NASA), “SLS-SPEC-159, Cross-Program Design Specification for Natural Environments (DSNE), Revision I”, Oct. 27, 2021.

[4] “Die Casting Cost: Control & Calculate Tooling and Mold Cost for Die Cast Parts.” *Moldie Casting*, https://moldiecasting.com/blog/die-casting-cost-control-calculate-tooling-and-mold-cost-for-die-cast-parts/

[5] “Titanium in Aerospace.” *SAMaterials*, 10 Apr. 2024, www.samaterials.com/podcast/titanium-in-aerospace.html

Appendix B: Hand Calculations

Coupling Axial Force and Seal Compression Calculations

These hand calculations estimate both the axial force that the coupling will experience when pressurized to its maximum design pressure, as well as the estimated force to seal the unpressurized coupling. The coupling axial force is calculated as if the coupling were at its maximum pressure of 650 psi and sealed on both ends. It is the product of the flow area times the pressure within the coupling. The force to compress the seal is calculated by finding the strain of the seal, multiplying that by the Youngs modulus to find the stress on the seal, and finally multiplying that by the seal area to find the required force to compress the seal. The seal is modelled as an annulus to simplify the calculation, which gives a conservative estimate, as the stress area of the annulus is greater than that of an O-ring. The Youngs modulus of a stiff rubber O-ring is used, once again giving a conservative estimate. Because we are using a spring energized seal, an accurate Youngs modulus could not be found, but we feel that these assumptions will give us a safe estimate of the sealing force.

COUPLING AXIAL FORCE

MAX PRESSURE, $P_{MAX} = 1000$ PSI
FLOW AREA DIAMETER, $d = 0.9$ in

$F_{AXIAL,MAX} = \frac{\pi}{4} d^2 \cdot P_{MAX}$

$F_{AXIAL,MAX} = \frac{\pi}{4} (0.9\,in)^2 \cdot 1000 \frac{lbf}{in^2}$

$F_{AXIAL,MAX} = 636.2\ lbf$

SEAL COMPRESSION FORCE
ASSUMPTIONS:
- ISOTROPIC, LINEAR ELASTIC
- SEAL MODELED AS EXTRUDED ANNULUS
- SEAL MODELED AS SOLID RUBBER

$E = 15\,MPa$
$d = 50\,mm$
$D = 57\,mm$
$t = 4.37\,mm$
COMPRESSION, $x = 1.25\,mm$

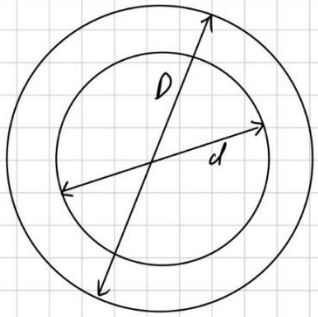

$\varepsilon = \frac{x}{t} = 0.286$

$A = \frac{\pi}{4}(D^2 - d^2) = 588.3\,mm^2$

$\sigma = E\varepsilon = 4.29\,MPa$

$F = \sigma A = 2.52\,KN \approx 566.5\,lbf$

Fluid Pressure Drop Calculations

Assumptions

The analysis assumes steady-state, fully developed internal flow through a rigid passage of constant internal diameter (0.75 in). Fluid properties were evaluated at constant temperature. Liquids were treated as incompressible, air was modeled as an ideal gas for density determination, and sludge was modeled as a Newtonian fluid.

Modeling Methodology

Major pressure losses were calculated using the Darcy–Weisbach relation:

$$\Delta P = f\left(\frac{L}{D}\right)\left(\frac{\rho V^2}{2}\right)$$

Minor losses, including entrance, exit, contraction, and expansion effects, were neglected in this first-order model. This simplification is justified because the coupling flow path is predominantly straight with constant diameter and an effective L/D ≈ 6.7 (5 in length, 0.75 in diameter). Under these conditions, distributed friction dominates and the resulting ΔP values represent a conservative lower-

bound estimate. Minor-loss terms can be incorporated in a subsequent refinement if required. The Darcy friction factor was determined from Reynolds number. Laminar cases used $f = 64/Re$, while turbulent cases used the Swamee–Jain explicit approximation to the Colebrook equation.

Reynolds Number and Flow Regime

All cryogenic and water cases are strongly turbulent. Sludge cases transition into laminar flow due to elevated viscosity, resulting in substantially increased friction factors.

For all low-viscosity fluids (water and cryogens), pressure drop across the coupling remains below approximately 0.4 psi at 30 GPM, corresponding to $C_v \approx 49–56$. This confirms that the coupling introduces minimal hydraulic restrictions under nominal operating conditions. As expected, the high-viscosity worst-case sludge scenario produces a significant pressure rise (≈81 psi) due to laminar-dominated flow and elevated friction factor. This case establishes an upper-bound hydraulic loading condition for structural and sealing evaluations.

Conversion to Flow Coefficients

For incompressible fluids, equivalent flow coefficients were determined using the standard relation:

$$C_v = \frac{Q}{\sqrt{\Delta P / SG}}$$

Assumptions	Parameters and Internal Coupling Dimensions		
1) Steady-state flow	Flowrate	30.000000	gal/min
2) Fully developed internal flow		0.066841	ft^3/s
3) Pipe is rigid & has constant ⌀	Length of Pipe	5.000000	in
4) Temperature is constant		0.416667	ft
5) Liquids treated as incompressible	Diameter (Constant)	0.750000	in
6) Air treated as an ideal gas		0.062500	ft
7) Sludge modeled as Newtonian fluid	Cross Sectional Area	0.003068	ft^2
Modeling	Inlet Fluid Velocity	21.786616	ft/s
1) Darcy-Weisbach EQ for ΔP calcs	Absolute Surface Roughness (Aluminum)	0.000005	ft
2) Swamee-Jain Correlation for "f"	Gravitational Constant	32.174000	lbm*ft/(lbf*s^2)
3) Minor losses neglected	Upstream/inlet gage pressure	1000	lbf/in^2
4) Entrance and exit losses neglected for straight pipe	Upstream/inlet absolute pressure	1014.7	lbf/in^2

	Air (20°C)	Water (20°C)	Liquid hydrogen (20 K)
Density_rho (lbm/ft^3)	3.391326531	62.3	4.4
Viscosity_u (lb*s/ft)	0.00000038	0.000021	0.00000027
Viscocity_v (ft^2/s)	0.00016	0.0000108	0.000002
Reynolds #	8510.396779	126079.9523	680831.7423
Flow Type	Turbulent	Turbulent	Turbulent
Friction Factor	0.032524728	0.017569112	0.013722705
Dynamic Pressure (PSI)	25.01578307	459.5497576	32.45616265
Pressure Drop (PSF)	5.424210241	53.82587382	2.969242262
Pressure Drop (PSI)	0.037668127	0.37379079	0.020619738
SG	1	1	0.071
Cv	1.425003391	49.06897163	55.6684153

	Liquid oxygen (90 K)	Sludge (realistic case of 2% Solids)	Sludge (worst case of 10% Solids)
Density_rho (lbm/ft^3)	71	62.99	65.89
Viscosity_u (lb*s/ft)	0.0000042	0.00167	0.157
Viscocity_v (ft^2/s)	0.0000019	0.000853	0.0765
Reynolds #	716664.9919	1596.32296	17.79952268
Flow Type	Turbulent	Laminar	Laminar
Friction Factor	0.013646519	0.040092138	3.595602038
Dynamic Pressure	523.7244428	464.639474	486.0310358
Pressure Drop (PSF)	47.64677136	124.1892653	11650.49455
Pressure Drop (PSI)	0.330880357	0.862425454	80.90621215
SG	1.14	1.01	1.06
Cv	55.68499536	32.46542995	3.433865282